Control of neurulation by the nucleosome assembly protein-1–like 2

Ute C. Rogner[1], Demetri D. Spyropoulos[3], Nicolas Le Novère[2], Jean-Pierre Changeux[2] & Philip Avner[1]

Neurulation is a complex process of histogenesis involving the precise temporal and spatial organization of gene expression[1,2]. Genes influencing neurulation include proneural genes determining primary cell fate, neurogenic genes involved in lateral inhibition pathways and genes controlling the frequency of mitotic events. This is reflected in the aetiology and genetics of human and mouse neural tube defects, which are of both multifactorial and multigenic origin[3]. The X-linked gene *Nap1l2*, specifically expressed in neurons, encodes a protein that is highly similar to the nucleosome assembly (NAP) and SET proteins. We inactivated *Nap1l2* in mice by gene targeting, leading to embryonic lethality from mid-gestation onwards. Surviving mutant chimaeric embryos showed extensive surface ectoderm defects as well as the presence of open neural tubes and exposed brains similar to those observed in human spina bifida and anencephaly. These defects correlated with an overproduction of neuronal precursor cells. Protein expression studies showed that the Nap1l2 protein binds to condensing chromatin during S phase and in apoptotic cells, but remained cytoplasmic during G1 phase. Nap1l2 therefore likely represents a class of tissue-specific factors interacting with chromatin to regulate neuronal cell proliferation.

The NAP-1 gene family has been implicated in the control of mitotic events[4,5]. NAP-1 assembles nucleosomes[6,7], acts as a core histone chaperone[8,9] and controls mitotic events by interaction of its SET domain with cyclins[10]. The mouse X-linked gene *Nap1l2*, and its human homologue *NAP1L2*, are mainly expressed in the nervous system[11], suggesting an effect on nucleosome assembly or cell-cycle regulation specific to neural function.

To obtain a precise overview of the *Nap1l2* expression profile, we performed RNA *in situ* hybridization on sections of mouse embryos and adult mouse brain (Fig. 1*a*,*c*). *Nap1l2* expression was first detected at embryonic day (E) 10.5, which correlates with the onset of neuronal differentiation in the central and peripheral nervous systems (Fig. 1*a*). Differentiated regions within the nervous system showed strong labelling, whereas ventricular zones showed reduced signals (Fig. 1*b*). We conclude that *Nap1l2* is mainly expressed in neurons, and most strongly in post-mitotic neurons.

We created a null mutation of *Nap1l2* in male embryonic stem cells by homologous recombination. The intron-less gene was partly replaced by a β-galactosidase reporter and a neomycin resistance gene. Two independent *Nap1l2*$^{-/-}$ ES cell lines, 5b17 and 8b21, were used for blastocyst injection and morula aggregation.

From 153 chimaeric blastocysts, we obtained 34 pups, of which only 3 were low-percentage chimaeras as judged by coat colour. We obtained 37 newborns from 16 morula aggregation experiments that were similarly low-percentage chimaeras. Neither highly chimaeric live animals nor germline transmission was found.

In the context of an X-linked gene, prenatal lethality was not unlikely. We therefore examined embryos from CD-1 and C57BL/6 morula aggregations at different time points after reimplantation (Figs 2 and 3). We found a large number of resorptions between E12.5 and E14.5, whereas retarded embryos were mainly

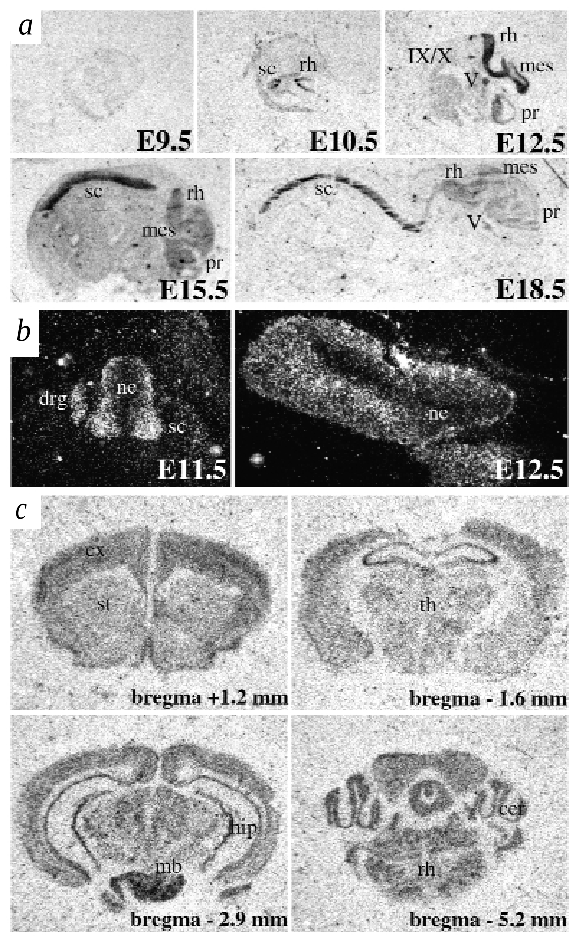

Fig. 1 Localization of *Nap1l2* mRNAs in the mouse nervous system by *in situ* hybridization with oligonucleotide probes. ***a***, Bright-field photographs of film autoradiograms showing *Nap1l2* expression at different developmental stages. The expression domain covers all structures of the nervous system, the neural tube and the peripheral ganglia. ***b***, Dark-field microphotographs of emulsion autoradiograms, showing details of *Nap1l2* expression in the nervous system. Left, expression at the lumbar level in the E11.5 spinal cord and peripheral ganglia. Note the more extensive labelling in the ventral region due to the ventro-dorsal differentiation gradient, also visible at E15.5 on the corresponding autoradiogram. Right, expression in the E11.5 superior colliculus. Here again the ventricular zone is devoid of labelling. ***c***, Bright-field photographs of film autoradiograms showing *Nap1l2* expression in the adult mouse brain. Expression is widespread throughout the brain, but the intensity of staining is not correlated with cell density, suggesting variable expression. Note the strong labelling of the mammillary bodies. V, trigeminal ganglion; IX/X, ganglionic complex of the IX and X nerves; cer, cerebellum; cx, cortex; drg, dorsal root ganglion; hip, hippocampus; mb, mammillary bodies; mes, mesencephalon; ne, neuroepithelium; pr, prosencephalon; rh, rhombencephalon; sc, spinal cord; st, striatum; th, thalamus.

[1]Génétique Moléculaire Murine CNRS URA 1947 and [2]Neurobiologie Moléculaire CNRS URA 1284, Institut Pasteur, Paris Cedex 15, France. [3]Center for Molecular and Structural Biology, Medical University of South Carolina, Charleston, South Carolina, USA. Correspondence should be addressed to U.C.R. (e-mail: urogner@pasteur.fr).

© 2000 Nature America Inc. • http://genetics.nature.com

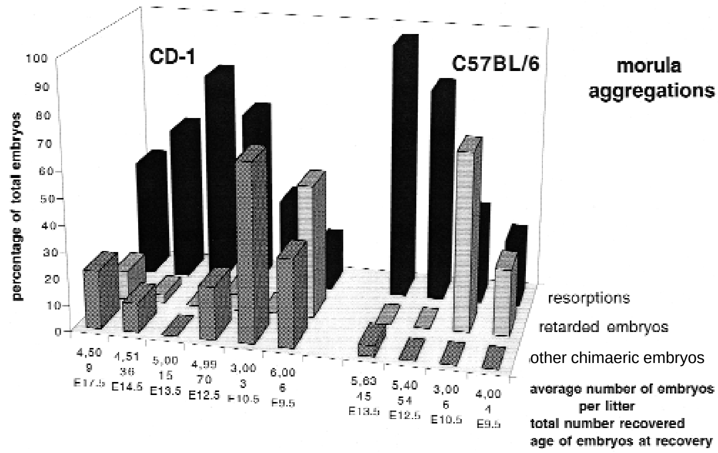

Fig. 2 Chimaeric, retarded and resorbed embryos at different time points during mouse development. Average numbers of embryos obtained in morula aggregation experiments are given as percentages of total embryos recovered. Under other 'chimaeric embryos' are included all live chimaeric embryos recovered that were not visibly retarded. Embryos obtained from the CD-1 and C57BL/6 experiments are listed seperately. Each foster mother was implanted with 8–12 morulas.

observed between E9.5 and E10.5, probably corresponding to the resorptions found at later embryonic stages (Fig. 2). In general, we recovered fewer embryos from the C57BL/6 morula aggregation experiments (Fig. 2), suggesting that genetic background may be an important factor in determining the severity of the phenotype.

We first detected nuclear localization motif (NLS) -*lacZ* expression in normally developed embryos in the caudal tip of the tail at E9.5 (Fig. 3). Expression extended to the entire neural tube by E10.5. E12.5 embryos showed *lacZ* labelling within the neural tube and the ganglia, and to a lesser extent in some muscles of the upper and lower thoracic regions (Fig. 3*a–c*, E12.5). The phenotype in these embryos was highly reproducible. All chimaeric embryos had defects in the surface ectoderm characterized by failure of neural tube closure, typically in the upper and lower thoracic regions (Fig. 3*a–c*). The percentage of chimaerism determined by *lacZ* staining correlated with the severity of the neural tube defect (Fig. 3*a*,*b*, E12.5).

We next analysed sections of embryonic tissue (Fig. 4). Strong *lacZ* expression in the rhombencephalon and the spinal cord correlated with the failure of neural tube closure at this position (Fig. 4*a*,*c*). Often, the surface ectoderm and the spinal cord were detached from the rest of the body (Fig. 4*a*,*e*). Staining of *lacZ* was generally fainter in the brain than in the spinal cord. Large parts of the brain, including telencephalon, diencephalon and mesencephalon, were expanded (Fig. 4*b*). These neural tissues were disorganized, and separation of neuroepithelium and neurons was barely detectable. Immunolabelling with antibodies against neuronal marker proteins demonstrated that most overproduced cells corresponded to nestin-positive neuronal precursor cells. At E14.5, the appropriate parts of the brain appeared necrotic (Fig. 4*g*), and anencephaly was found in chimaeric E17.5 embryos (Fig. 3).

We observed a second associated phenotype at E13.5 and E14.5. Two chimaeric E13.5 embryos showed overdevelopment of the entire *lacZ*-stained surface ectoderm. One well-developed E14.5 chimaeric embryo had the skin on its back detached (Figs 3, top, E14.5 embryo, and 4*f*,*h*). No phenotype was associated with *lacZ* expression in other tissues.

The *in vivo* results suggest that the absence of *Nap1l2* leads to an overproduction of cells derived from neuroectoderm. *In vitro*, ES cells differentiate on formation of embryoid bodies in suspension culture. Re-attachment of the embryoid bodies after four days of culture leads to the formation of various types of differentiated cells. Formation of neurons can be increased by the addition of retinoic acid to the medium[12,13]. We used antibodies directed against various neuronal marker proteins to visualize the specific cell types formed: nestin, which is present in precursor cells; β-tubulin III, in early neurons; NF200, in differentiated neurons; and GFAP, in glial cells. The original ES-cell line CK35 and the mutant cell lines 5b17 and 8b21 were able to form neurons in the presence of retinoic acid in similar numbers and kinetics (data not shown). We found NLS-*lacZ* expression (allowing us to follow *Nap1l2* promoter activity in the mutant cell lines) mainly in mature neurons, but also in nestin-positive precursor cells.

In the absence of retinoic acid, the original cell line produced relatively few neuronal cells. In contrast, the mutant cell lines produced large numbers of nestin-positive neuronal cells increasing from about 50 cells per mm^2 one day to 200 cells per mm^2 three days after re-attachment (Fig. 5*a*,*b*). Many of these

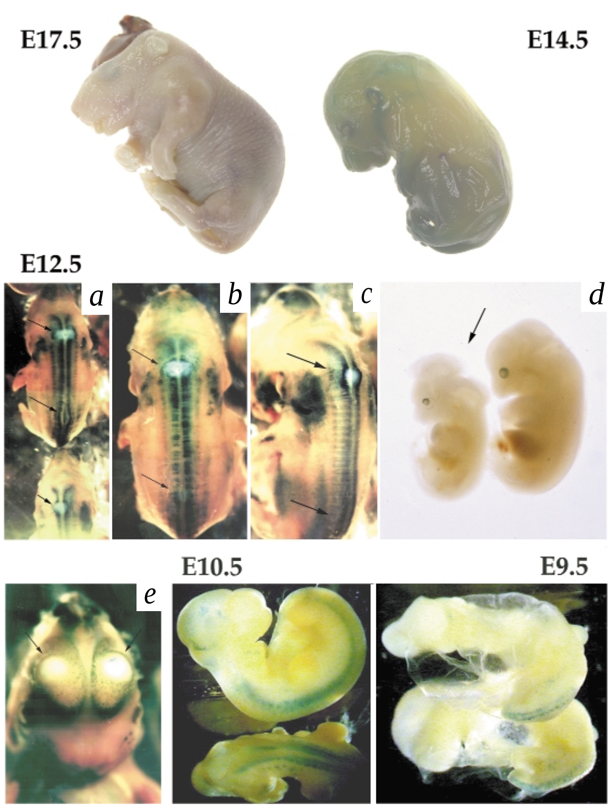

Fig. 3 Mutant chimaeric embryos obtained from morula aggregation experiments. The E17.5 embryo (CD-1 morula aggregate) is one of two embryos found in the same experiment that exhibited anencephaly. The E14.5 embryo is a high percentage chimaeric CD-1 aggregate with dark eye pigmentation that shows detached surface ectoderm. In experiments using CD-1 morulas, we found 14 non-resorbed chimaeric embryos, including six that displayed *lacZ* staining predominantly along the dorsal midline. The E12.5 embryos shown here are representative of the ectoderm defects found (arrows): ***a***,***b***,***c***, open neural tube; ***d***, hindbrain ablation. ***e***, Exposed telencephalon. A control embryo is shown on the right side of (*d*). The apparently normal E10.5 chimaera has *lacZ* staining along its entire dorsal length. The two apparently normal E9.5 chimaeras show *lacZ* staining restricted to the very caudal tip of the tail.

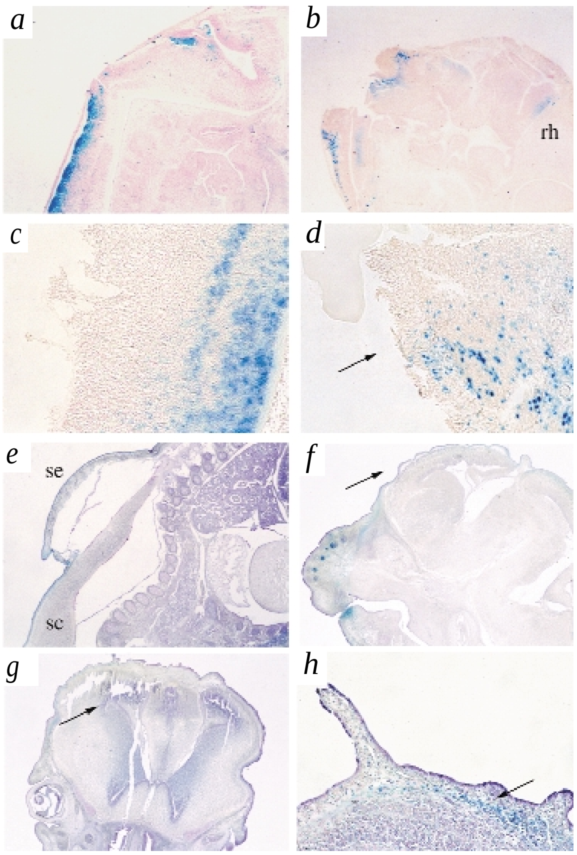

Fig. 4 Sections of *lacZ*-stained embryos with specific phenotypes. ***a***, Section of an E12.5 embryo with an open neural tube defect (arrow) in the upper thoracic region. ***b***, Strong rearrangements of the brain of an E12.5 embryo. The position of the rhombencephalon is indicated (rh). ***c***, Exposed neural tube (E12.5, compare with *a*). ***d***, Exposed neural tissue (arrow) of the brain (E12.5, compare with *b*). ***e***, Detached surface ectoderm (se) and spinal cord (sc) at E13.5. ***f***, Overproduction of surface ectoderm (arrow) at E13.5. Note also the *lacZ* staining in the virbrissa. ***g***, Possible necrosis (arrow) in the brain of a chimaeric E14.5 embryo. ***h***, Overproduction of surface ectoderm and *lacZ* staining in the underlying mesenchyme (arrow) at E14.5.

nestin-positive cells were *lacZ* positive (Fig. 5*c*). Pulse–chase experiments using BrdU confirmed that these *lacZ* expressing cells represent a growing cell population (data not shown).

We conclude from these experiments that the *Nap1l2* mutation affects the proliferation of neuronal precursor cells *in vivo* as well as *in vitro*. The dual effect of retinoic acid on both neuronal cell differentiation and G1 arrest of cell division[13] probably leads to the suppression of the proliferative effect of the *Nap1l2* mutation.

To understand the function of Nap1l2 protein in proliferating cells, we studied its localization in P19 embryonal carcinoma cells[14] (EC), which also express *Nap1l2*. We cloned the coding sequence of *Nap1l2* into the pEGFP-C1 vector allowing expression of GFP fusion proteins under the control of the CMV promoter. On transfection of subconfluent P19 cell cultures, Nap1l2 localizes to the cytoplasm or to both the nucleus and the cytoplasm. Cell-cycle arrest experiments showed that the protein is cytoplasmic in the G1 phase (Fig. 6*a*), whereas localization in the nucleus occurs in cells that enter S phase (Fig. 6*b*). DAPI staining indicated co-localization of Nap1l2 in regions of the nucleus with high chromatin density. When cells expressing Nap1l2 were kept subconfluent and growing, almost all of the Nap1l2-positive cells became apoptotic and died within 24 hours. Nap1l2 protein remained associated with chromatin in apoptotic cells (Fig. 6*c*). In contrast, Nap1l2-expressing cells arrested in G1 phase survived in culture and few of these cells became apoptotic. Similar results were observed on overexpression of the unfused Nap1l2 protein, but not on overexpression of GFP alone (data not shown). When placed under the control of the *Nap1l2* promoter, GFP-Nap1l2 similarly localized to the cytoplasm during G1 phase. Cells that expressed Nap1l2 in the nucleus after replication showed condensation of the replicated chromatin, often associated with apoptosis (Fig. 6*d*–*g*).

A possible mechanism for Nap1l2 function is suggested by its interaction with condensing chromatin. Upregulation of Nap1l2 expression concomitant with neuronal differentiation may slow down cell division or lead to cell-cycle arrest, or eventually to apoptosis, a key mechanism regulating the elimination of neuronal precursor cells during mammalian brain development[15]. Like other ubiquitously expressed proteins, Nap1l2 may participate in chromatin remodelling that can be directly correlated to the frequency of cell division[16,17]. The importance of cell proliferation in neural tube closure has been shown by, for example, mutations in *Hes1* and *Pax3*, which correlate with changes in rates of cell division in neural tissues[18,19].

Closer examination of the role of *Nap1l2* and *NAP1L2* in neuronal cell-cycle regulation should provide novel insights into the development processes and the aetiology of neural tube defects in mouse and human[20]. In humans, heritability for anencephaly and spina bifida is approximately 60% (ref. 3), and genetic background clearly influences the penetrance of mouse neural tube defects[21,22]. Differences in the phenotypic severity of the *Nap1l2* mutation, dependent on genetic background, could be used to identify modifier genes once conditional *Nap1l2*-mutant strains become available.

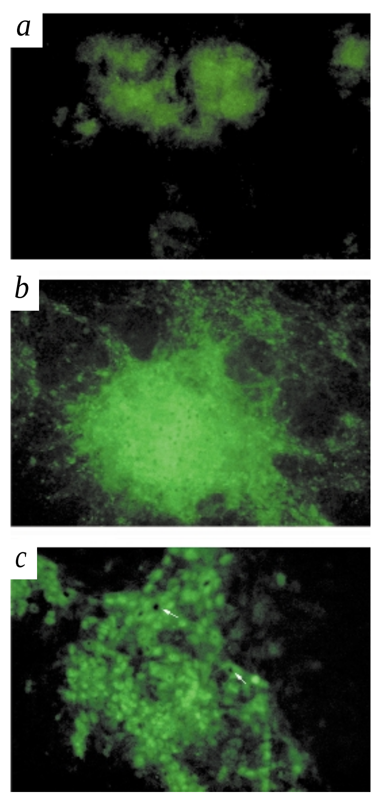

Fig. 5 ES cells from the mutant ES cell line 5b17 differentiate *in vitro* into neurons. *a*–*c*, Photos of immunofluorescence using anti-nestin antibodies. The normal cell line CK35 (***a***) and the mutant cell line 5b17 (***b***) on day 9 of *in vitro* differentiation are shown. ***c***, *lacZ*-positive cells (arrows) within the nestin-positive cell population.

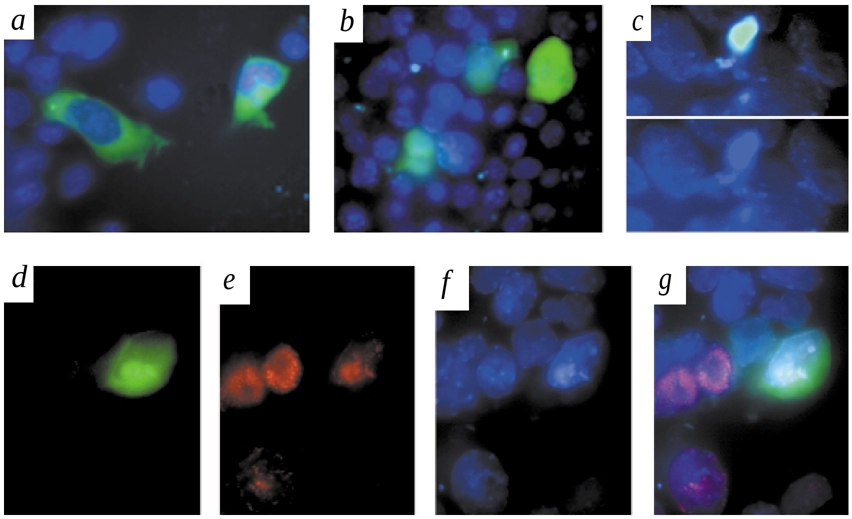

Fig. 6 P19 cells transfected with the expression vector pEGFP express GFP–Nap1l2 fusion proteins under the control of the CMV promoter (*a*–*c*). The cells are counterstained with DAPI. Nap1l2 localizes to the cytoplasm of cells arrested in G1 phase (***a***; growth in medium with 0.5% FCS for 72 h), to the nucleus of cells arrested in S phase (***b***; 10^{-7} M methotrexate for 24 h), and Nap1l2 localizes to the condensed chromatin in cells undergoing nuclear fragmentation (***c***). The lower panel shows the DAPI counterstaining of (*c*). *d*–*g*, Expression of the GFP fusion protein under the control of the endogenous *Nap1l2* promoter. ***d***, Cell expressing the Nap1l2 fusion protein during or after S phase show chromatin condensation. ***e***, BrdU staining of (*d*). ***f***, DAPI staining of (*d*). ***g***, Merge of (*d*), (*e*) and (*f*).

Methods

In situ hybridization. We carried out *in situ* hybridization as described[23,24]. A 45mer oligonucleotide (5′–TTATCACAGTCACATACAATCAGAAGC CTTGCACTAGCTGTTATC–3′) was chosen from the 3′ UTR of *Nap1l2*. The temperature of the stringent rinse step was 45 °C. Labelling specificity was verified by displacement of labelled oligonucleotide with an excess of unlabelled probe.

Construction of mutant ES cells. We used *Nap1l2* cDNA to screen a 129/Sv genomic phage library in λ Dash II (Stratagene). Six phages were identified and analysed by single and double restriction digests with eight different enzymes. The restriction pattern of the phage DNAs was compared with that of genomic DNA. The insert of one of the phages was subcloned into pBluescript SK(+) (Stratagene) using *Not*I and *Xho*I. A deletion in *Nap1l2* was generated using the enzyme *Hin*cII followed by intramolecular religation. This eliminated 890 bp of coding sequence. Religation created a unique *Sal*I site, which was then used to insert in-phase a β-galactosidase reporter gene and a neomycin resistance gene. The cloning of these cassettes disrupted the reading frame of the remaining *Nap1l2* sequence. The resulting fusion protein has no potential for Nap1l2 function, because it includes only five amino acids from the amino-terminal end of Nap1l2. All the non-deleted carboxy-terminal sequences are out of frame. Finally, we inserted a HSV-*tk* cassette into the polylinker of the vector. The mutant construct was transfected into the ES cell line CK35 (a male 129/Sv cell line obtained from C. Kress and C. Babinet) and transfected clones were selected with geneticin (G418) and ganciclovir. Southern-blot analysis for screening of putative recombinants was optimized using the E18s single-copy probe flanking the construct, which was isolated from overlapping λ clones[25]. Two clones showed the expected restriction pattern for correct integration of the βGalNeo-cassette into *Nap1l2*. The absence of a *Nap1l2* transcript was confirmed by RT–PCR and the presence of an unmodified karyotype by examination of mitotic spreads. Both clones were used for microinjection into C57BL/6 blastocysts[26] and morula aggregation experiments using either C57BL/6 or CD-1 morulas.

Morula aggregation. We performed morula aggregation experiments as described[27,28]. Embryos were obtained from 3–5-week-old females injected intraperitoneally with PMSG (5 IU) then 46 h later with hCG (5 IU), and immediately mated with stud males. Females were checked for plugs the following morning, noon of this day being considered as E0.5. We killed positive females at E2.5 by cervical dislocation and isolated the female reproductive tract into PBS. Morulas were isolated by flushing oviducts using a blunt 30-gauge needle and M2 media. Zona pellucidas were removed by brief incubation in Acid Tyrodes. Compacted and non-compacted morulas were then transferred singly or in pairs into wells of tissue culture dishes containing M16 media under mineral oil. Feeder-free, ES-cell clumps (5–8 ES cells) from partially trypsinized ES-cell colonies were added to wells containing morulas and incubated for 4 h in a 37 °C, 5% CO_2 humidified incubator. ES cell/morula aggregates were then transferred to fresh tissue culture dishes containing M16 media under mineral oil and incubated overnight. We implanted 8–12 expanded blastocysts into the uterine horns of each anaesthetized E2.5 foster mother, each of which had been mated with vasectomized males.

Whole-mount X-gal staining of embryos. We carried out X-gal staining of embryos as described[29]. This procedure is ideally suited for E10.5 embryos. For older embryos, incubation times were lengthened accordingly. Embryos were dissected into PBS. The PBS was then replaced by a solution of 0.5% glutaraldehyde in PBS and the embryos shaken for 30 min at RT. After three successive rinses with PBS for a total of 30 min, the PBS was replaced by the staining solution (PBS containing 10 mM potassium ferrocyanide, 10 mM potassium ferricyanide, 1 mM spermidine, 2 mM $MgCl_2$, 0.02% NP-40, 0.01% sodium deoxycholate and 0.05% X-gal). Overnight incubation was at 30 °C, followed by rinsing in PBS and fixation in 3.7% formaldehyde in PBS for several h.

Histological survey. The embryos were either frozen in dry-ice powder, cryostat sectioned (14-μm sections), mounted on Superfrost+ slides and stored at –80 °C, or dehydrated immediately through an alcohol gradient, immersed in xylene, xylene/paraffin (1:1) and embedded in paraffin before microtome sectioning. X-gal staining of frozen sections was performed as described[30]. All sections were counterstained with either haematoxylin or toluidine blue. After dehydration through ethanol series, the slides were immersed in Histoclear (Prolabo) and mounted in Eukitt (Prolabo).

Differentiation of ES cells. Differentiation *in vitro* was carried out as described[12]. For proliferation studies, BrdU (10 μM; Sigma) was added to the medium for 1 h. Anti-BrdU antibody was from the DSHB.

Immunolabelling. Fixation was carried out for 20 min in 2% paraformaldehyde, followed by a PBS rinse and by permeabilization with 0.02% Triton X-100 for two min. After three further PBS rinses for five minutes, we incubated the slides for 1 h at 37 °C with the diluted antisera. PBS dilutions were as follows: anti-β-tubulin III, 1/400 (Sigma T-8660); anti-GFAP, 1/200 (DAKO Z03345); anti-NF200, 1/200 (Sigma N-4142); and anti-nestin antibody, 1/200 dilution (Rat-401 from the Developmental Studies Hybridoma Bank, University of Iowa). Secondary FITC- or Cy3-labelled antibodies (Nordic, Caltag) were used at a 1/300 dilution. After rinsing in PBS as above, slides were mounted in 2% n-propylgallate in glycerol. β-gal staining was performed after fixation and three rinses in PBS as described above.

For sections, primary antibodies were incubated overnight at 4 °C in a 1/80 dilution in PBS, 0.3% Triton X-100, 1% normal serum; secondary antibodies were used according to the manufactor's instructions (Amersham).

Protein expression studies. The coding sequence of *Nap1l2* was cloned into the *Xho*I and *Sma*I sites of the expression vector pEGFP-C1. Transfections into P19 cells were performed using lipotransfection (LipofectAMINE Plus from Gibco). GFP expression analysis was carried out 24 h after transfection using a fluorescence microscope and a standard illumination wavelength of 475 nm. Alternatively, the *GFP* coding sequence was inserted into the *Sal*I site at the 5´-end of the *Nap1l2* coding sequence which was contained in a genomic fragment covering *Nap1l2* in its entirety.

Acknowledgements

We thank Y. Gong for technical assistance; C. Rougeulle for DNA probes; M. Cohen-Tannoudji for the lacZneo cassette; A. Copp and P. Stanier for comments concerning the mutant phenotypes; A. Prochiantz and D. Riethmacher for advice on antibodies; and E. Heard for critical reading of the manuscript. U.C.R. has been supported by grants from the Deutsche Forschungsgemeinschaft, the AFM and the EEC (contract no. BMH4-CT98-5072). D.D.S. was supported for this research by URRF Gene Targeting/Knockout Mouse Facility funding. N.L. was financed by the Ministère de la Recherche et de l'Enseignement, AFM and the Pasteur Institute J.P.C. was supported by the Collège de France and AFM.

Received 24 September 1999; accepted 17 May 2000.

1. Kerszberg, M. & Changeux, J.-P. A simple molecular model of neurulation. *Bioessays* **20**, 758–770 (1998).
2. Wilson, P.A. & Hemmati-Brivanlou, A. Vertebrate neural induction: inducers, inhibitors, and a new synthesis. *Neuron* **18**, 699–710 (1997).
3. Emery, A.E.H. in *Methodology in Medical Genetics* 58 (Churchill Livingstone, Edinburgh, 1986).
4. Altman, R. & Kellog, D. Control of mitotic events by Nap1 and Gin4 kinase. *J. Cell Biol.* **138**, 119–130 (1997).
5. Simon, H.U. *et al.* Molecular characterization of *hNRP*, a cDNA encoding a human *nucleosome-assembly-protein-I-related* gene product involved in the induction of cell proliferation. *Biochem. J.* **297**, 389–397 (1994).
6. Laskey, R.A., Honda, B.M., Mills, A.D. & Finch, J.T. Nucleosomes are assembled by an acidic protein which binds histones and transfers them to DNA. *Nature* **275**, 416–420 (1978).
7. McQuibban, G.A., Commisso-Cappelli, C.N. & Lewis, P.N. Assembly, remodeling, and histone binding capabilities of yeast nucleosome assembly protein 1. *J. Biol. Chem.* **273**, 6582–6590 (1998).
8. Ito, T., Bulger, M., Kobayashi, R. & Kadonaga, J.T. Drosophila NAP-1 is a core histone chaperone that functions in ATP-facilitated assembly of regularly spaced nucleosomal arrays. *Mol. Cell. Biol.* **16**, 3112–3124 (1996).
9. Rodriguez, P. *et al.* Functional characterization of human *nucleosome assembly protein-2* (*NAP1L4*) suggests a role as a histone chaperone. *Genomics* **44**, 253–265 (1997).
10. Kellogg, D.R., Kikuchi, A., Fujii-Nakata, T., Turck, C.W. & Murray, A.W. Members of the NAP/SET family of proteins interact specifically with B-type cyclins. *J. Cell Biol*. **130**, 661–673 (1995).
11. Rougeulle, C. & Avner, P. Cloning and characterization of a murine brain specific gene *Bpx* and its human homologue lying within the *Xic* candidate region. *Hum. Mol. Genet*. **5**, 41–49 (1996).
12. Fraichard, A. *et al. In vitro* differentiation of embryonic stem cells into glial cells and functional neurons. *J. Cell Sci.* **108**, 3181–3188 (1995).
13. Struebing, C. *et al.* Differentiation of pluripotent embryonic stem cells into the neuronal lineage *in vitro* gives rise to mature inhibitory and excitatory neurons. *Mech. Dev.* **53**, 275–287 (1995).
14. McBurney, M.W. P19 embryonal carcinoma cells. *Int. J. Dev. Biol.* **37**, 135–140 (1993).
15. Naruse, I. & Keino, H. Apoptosis in the developing CNS. *Prog. Neurobiol.* **47**, 135–155 (1995).
16. Khochbin, S. & Wolffe, A.P. Developmentally regulated expression of linker-histone variants in vertebrates. *Eur. J. Biochem.* **225**, 501–510 (1994).
17. Reyes, J.C. *et al.* Altered control of cellular proliferation in the absence of mammalian brahma (SNF2α). *EMBO J.* **17**, 6979–6991 (1998).
18. Ishibashi, M. *et al.* Targeted disruption of mammalian *hairy* and *Enhancer of split* homolog-1 (*HES-1*) leads to up-regulation of neural helix-loop-helix factors, premature neurogenesis, and severe neural tube defects. *Genes Dev.* **9**, 3136–3148 (1995).
19. Wilson, D.B. Proliferation in the neural tube of the *Splotch* (*Sp*) mutant mouse. *J. Comp. Neurol.* **154**, 249–256 (1974).
20. Jensson, O. *et al.* A family showing apparent X linked inheritance of both anencephaly and spina bifida. *J. Med. Genet.* **25**, 227–229 (1988).
21. Neumann, P.E. *et al.* Multifactorial inheritance of neural tube defects: localization of the major gene and recognition of modifiers in *ct* mutant mice. *Nature Genet.* **6**, 357–362 (1994).
22. Copp, A.J., Checiu, I. & Henson, J.N. Developmental basis of severe neural tube defects in the *loop-tail* (*Lp*) mutant mouse: Use of microsatellite DNA markers to identify embryonic genotype. *Dev. Biol.* **165**, 20–29 (1994).
23. Young, W.S. 3d, Bonner, T.I. & Brann, M.R. Mesencephalic dopamine neurons regulate the expression of neuropeptide mRNAs in the rat forebrain. *Proc. Natl Acad. Sci. USA* **83**, 9827–9831 (1986).
24. Le Novère, N., Zoli, M. & Changeux, J.P. Neuronal nicotinic receptor alpha 6 subunit mRNA is selectively concentrated in catecholaminergic nuclei of the rat brain. *Eur. J. Neurosci*. **8**, 2428–2439 (1996).
25. Rougeulle, C., Colleaux, L., Dujon, B. & Avner, P. Generation and characterization of an ordered λ clone array for the 460-kb region surrounding the murine *Xist* sequence. *Mamm. Genome* **5**, 416–423 (1994).
26. Gardner, R.L. Mouse chimeras obtained by the injection of cells into the blastocyst. *Nature* **220**, 596–597 (1968).
27. Wood, S.A. *et al.* Simple and efficient production of embryonic stem cell-embryo chimeras by coculture. *Proc. Natl Acad. Sci. USA* **90**, 4582–4585 (1993).
28. Nagy, A., Rossant, J., Nagy, R., Abramow-Newerly, W. & Roder, J.C. Derivation of completely cell culture-derived mice from early-passage embryonic stem cells. *Proc. Natl Acad. Sci. USA* **90**, 8424–8428 (1993).
29. Papenbrock, T. *et al.* Murine *Hoxc-9* gene contains a structurally and functionally conserved enhancer. *Dev. Dyn.* **12**, 540–547 (1998).
30. Hogan, B., Beddington, R., Costantini, F. & Lacy, E. in *Manipulation of the Mouse Embryo* 373–375 (Cold Spring Harbor Laboratory Press, New York, 1994).